論 文 15-2-5

Integrated Magnetic Transformer for ZVS Phase Shift Full Bridge Converter

Xin-Lan Li*, Yong-Hwan Shin**, Jae-Sun Won***, Jong-Sun Kim****,and Hwi-Beom Shin†

ABSTRACT

An integrated magnetic (IM) transformer is proposed for a phase shifted full bridge (PSFB) converter with zero voltage switching (ZVS). In a proposed IM transformer, the transformer is located on the center leg of E-core and the output inductor is wound on two outer legs with air gap. The proposed IM transformer is analyzed by using the magnetic capacitor model. For reducing the core size, EE core is redesigned. The proposed IM transformer is experimentally verified on a 1.2 kW prototype converter. The converter efficiency with the proposed IM transformer is about 93 % at full load and its volume size can be reduced. It can be expected that the power density can be largely increased with the proposed IM transformer.

Key Words : Power electronics, Integrated magnetic transformer, Full bridge converter

1. Introduction

The IM transformers begin to be used in the low output voltage and high current power electronics system [1-3]. With the IM technique, two or more magnetic components are integrated in one magnetic structure. The EE or EI core is commonly utilized. The magnetic parts in the converter may be reduced, so that the size and power density can be improved. In some case, overall efficiency may be increased and an EMI problem may be reduced.

For the PSFB converter, several IM transformers are proposed [1-4]. The transformer winding is typically located on the two outer legs in series connection and the inductor is wound on the center leg. The AC flux of transformer and a half of the DC flux of inductor flows in outer legs but the inductor flux only flows in the center leg. The flux density in outer leg is much higher than one in center leg because the center leg has nearly two time cross-sectional area of the outer leg. This IM transformer has a high magnetizing inductance and loose coupling between the primary and the secondary.

A new IM transformer is proposed for ZVS PSFB converter in this paper. The transformer winding is located on the center leg for close magnetic coupling and the inductor is wound on two outer legs in series connection. The proposed IM transformer is analyzed electrically and magnetically. An E-core is redesigned and implemented. The proposed IM transformer is experimentally verified through a 1.2kW prototype ZVS PSFB converter and the performance is discussed.

2. Proposed IM transformer for ZVS PSFB converter

The ZVS PSFB converter is shown in Fig. 1. The

†교신저자 : 정회원, 경상대 전기공학과 교수
E-mail : hbshin@gsnu.ac.kr
*학생회원, 경상대 전기공학과 박사과정
**학생회원, 경상대 전기공학과 박사과정
***정회원, 삼성전기(주) 책임연구원
****정회원, 삼성전기(주) 그룹장
접수일자 : 2010. 2. 3 1차 심사 : 2010. 2. 7
심사완료 : 2010. 3. 8

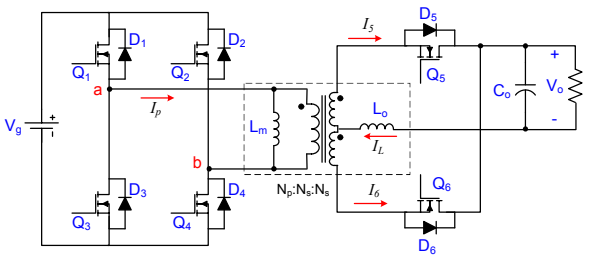

Fig. 1 ZVS PSFB converter

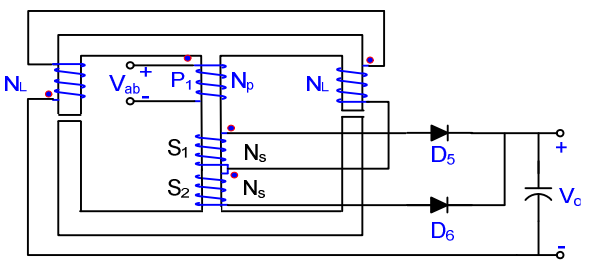

Fig. 2 Proposed integrated magnetic transformer

diodes D_1~D_6 denote the MOSFET body diodes and the synchronous rectifiers are used in the output of the center-tapped rectifier for high efficiency. The center-tapped transformer and the output inductor are magnetically integrated on single EE or EI core. Fig. 2 shows the proposed IM transformer and the circuit connection in the output stage. The transformer is located on the center leg and the output inductor is wound on two outer legs. The air gaps are inserted in the outer legs.

When the PSFB converter operates in ZVS, there are eight operating modes including powering, freewheeling, and zero-voltage switching transition modes during each PWM switching cycle [7]. The ZVS transition intervals are negligible for analyzing and designing the integrated magnetic circuit. Hence, four modes only are considered for analysis. Fig. 3 shows the phase-shift switching pattern and the voltage and current waveforms. The duty ratio d is limited below 0.5 because of the alternating current for transformer.

The magnetic states within each core leg are modelled by using the capacitive modelling method [5, 6]. For simplicity, it is assumed that all the devices are ideal and the core material has infinite permeance. The operation is explained in the following.

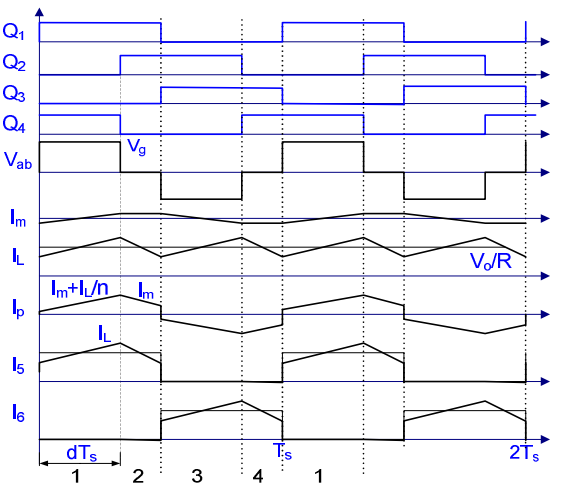

Fig. 3 Operational electrical waveforms

Mode 1 (powering): $0 < t < dT_s$

In Fig. 1, both Q_1 and Q_4 are turned on. This mode is shown in Fig. 4(a) where the thick line denotes the current flow. The primary voltage V_{ab} is positive and the secondary current flows through N_s,N_L,D_5, and the load. Fig. 4(b) shows the corresponding capacitor model. From Fig. 4, the flux rate equations in the core leg can be obtained as

$$\begin{aligned} &N_p\dot{\Phi}_c = V_g \\ &N_s\dot{\Phi}_c - N_L\dot{\Phi}_1 + N_L\dot{\Phi}_2 = V_o \\ &\dot{\Phi}_1 + \dot{\Phi}_2 = \dot{\Phi}_c \end{aligned} \tag{1}$$

where

$\dot{\Phi}_c$: flux rate of center leg
$\dot{\Phi}_1$: flux rate of right leg
$\dot{\Phi}_2$: flux rate of left leg
N_p: primary winding turns
N_s: secondary winding turns
N_L: inductor winding turns
V_g : input voltage
V_0 : output voltage

Solving (1) for three flux rates yields that

$$\dot{\Phi}_c = \frac{V_g}{N_p} \tag{2}$$

$$\dot{\Phi}_1 = \frac{1}{2}\left\{(1+N_s/N_L)\frac{V_g}{N_p} - \frac{V_0}{N_L}\right\} \tag{3}$$

$$\dot{\Phi}_2 = \frac{1}{2}\left\{(1-N_s/N_L)\frac{V_g}{N_p} + \frac{V_0}{N_L}\right\} \tag{4}$$

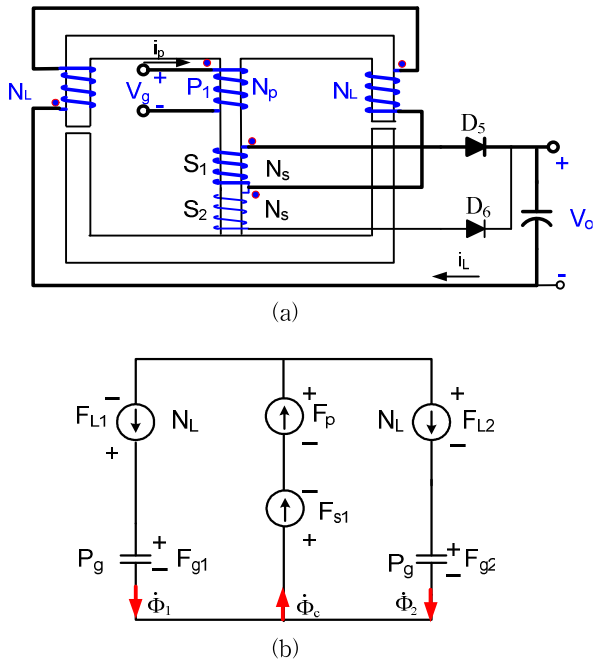

Fig. 4 Mode 1; (a) current flow, (b) capacitor model

The flux in the center leg increases linearly in Mode 1.

Mode 2 (free wheeling): $dT_s < t < 0.5T_s$

In this mode, both Q_1 and Q_2 are turned on after ZVS switching transition in Fig. 1. Mode 2 finished when Q_1 is turned off. The primary winding is freewheeling and the primary voltage is zero. The diode D_5 keeps conducting the inductor current. Mode 2 is similar to Mode 1 except the value of primary voltage, so that Fig. 4 can be used for this free wheeling mode. The flux rate in each leg can be expressed from (1) as

$$\dot{\Phi}_c = 0 \tag{5}$$

$$\dot{\Phi}_1 = -\frac{V_0}{2N_L} \tag{6}$$

$$\dot{\Phi}_2 = \frac{V_0}{2N_L} \tag{7}$$

The flux in the center leg keeps a constant value in Mode 2.

Mode 3 (powering): $0.5T_s < t < (0.5+d)T_s$

Both Q_2 and Q_3 in Fig. 1 are turned on. Mode 3 finishes when Q_2 is turned OFF. During Mode 3, the primary voltage V_g is negative and the secondary current flows through N_s, N_L, D_6, and the load as shown in Fig. 5(a). From Fig. 5(b), the following equations can be derived as

$$\begin{aligned} &N_p\dot{\Phi}_c = -V_g \\ &-N_s\dot{\Phi}_c - N_L\dot{\Phi}_1 + N_L\dot{\Phi}_2 = V_o \\ &\dot{\Phi}_1 + \dot{\Phi}_2 = \dot{\Phi}_c \end{aligned} \tag{8}$$

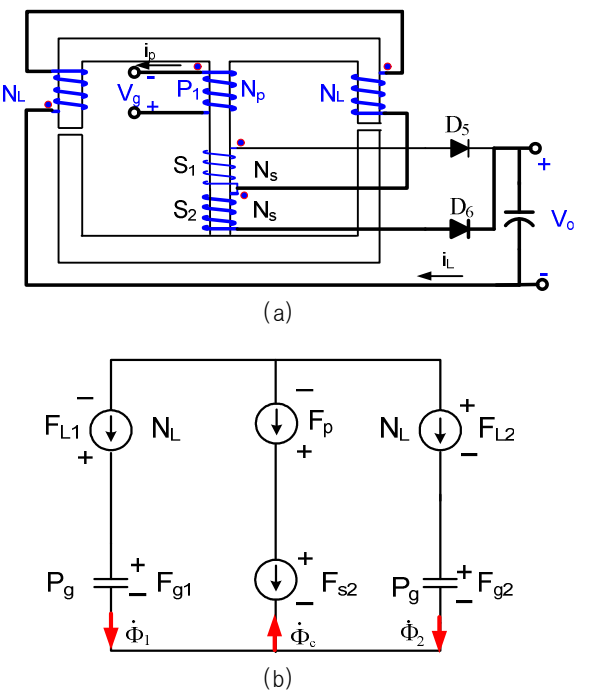

Fig. 5 Mode 3: (a) current flow, (b) capacitor model

Solving (8) for three flux rates yields that

$$\dot{\Phi}_c = -\frac{V_g}{N_p} \tag{9}$$

$$\dot{\Phi}_1 = -\frac{1}{2}\left\{(1-N_s/N_L)\frac{V_g}{N_p} + \frac{V_0}{N_L}\right\} \tag{10}$$

$$\dot{\Phi}_2 = -\frac{1}{2}\left\{(1+N_s/N_L)\frac{V_g}{N_p} - \frac{V_0}{N_L}\right\} \tag{11}$$

Mode 4(free wheeling): $(0.5+d)T_s<t<T_s$

In this model, both Q_3 and Q_4 are turned on in Fig.1. The primary winding is in the freewheeling state, so the primary voltage is zero. Because of the magnetizing current, D_6 keeps conducting with primary current. From (8) we can obtain equations:

$$\dot{\Phi}_c = 0 \tag{12}$$

$$\dot{\Phi}_1 = \frac{V_0}{2N_L} \tag{13}$$

$$\dot{\Phi}_2 = -\frac{V_0}{2N_L} \tag{14}$$

Fig. 6 shows the theoretical magnetic waveforms. The inductor in the outer legs should have a DC flux level for storing energy in the air gap but the transformer winding in the center leg has only AC flux. The average flux rate of the inductor winding should be zero during a PWM interval. The voltage conversion ratio can be derived, by averaging the flux rate in one inductor winding, as

$$M(D) = \frac{V_o}{V_g} = 2D\frac{N_s}{N_p} \tag{15}$$

where D is the steady state value of the duty ratio d. Then, the equivalent inductance of output inductor becomes

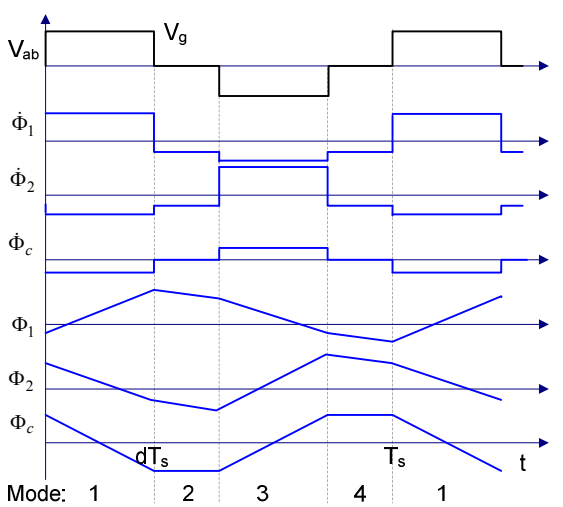

Fig. 6 Operational magnetic waveforms

$$L_o = 2N_L{}^2 P_g \tag{16}$$

P_g denotes the air gap permeance in a outer leg and it is given by

$$P_g = \frac{\mu_0 A_o}{l_g} \tag{17}$$

where A_o and LG are the cross-sectional area of outer leg and air gap length, respectively, and m_0 is permeability of air. The magnetizing inductance at the primary side can be found from Fig. 2(a) as

$$L_m = 2N_p{}^2 P_g \tag{18}$$

Therefore, the peak flux density in outer leg can be written as

$$B_{o,peak} = B_o + \frac{1}{2}\Delta B_o = \frac{N_L P_g}{A_o} I_L + \frac{1}{2}\cdot\frac{V_o}{4f_s A_o}\left(\frac{1}{N_s} + \frac{1-2D}{N_L}\right) \tag{19}$$

The peak flux density in the center leg can be derived as

$$B_{c,peak} = B_c + \frac{1}{2}\Delta B_c = \frac{V_o}{4f_s N_s A_c} \tag{20}$$

3. Simulation and experimental results

The design specification is shown in Table 1. A 1.2kW/12V full bridge dc-dc converter is designed and built to verify the analysis.

3.1 Core and winding design

For the transformer turns ratio 20:1:1, the duty ratio is D=0.3 for normal condition. The numbers of turns of transformer and output inductor are chosen as

$$N_p = 40, \qquad N_s = 2, \qquad N_L = 2$$

The core is made for this application. The core dimension is shown in Fig. 7 and the value of

Table 1 Circuit specification

Rated output power	1.2 kW
Input voltage	350 ~ 410 Vdc
Output voltage	12 Vdc
Switching frequency	100 kHz
Output inductance	0.656 mH
Turns ratio of transformer	20:1:1
Maximal flux density	0.2 T

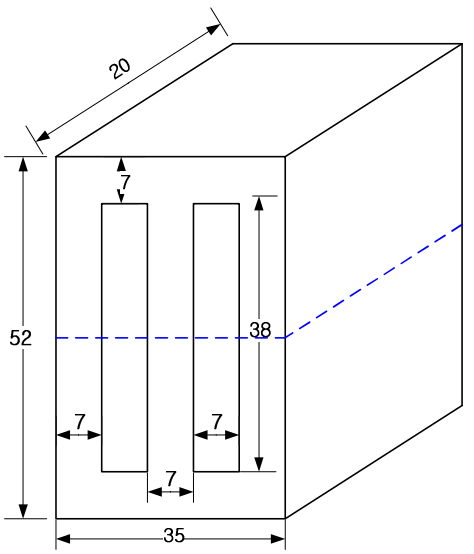

Fig. 7 EE core dimension in mm

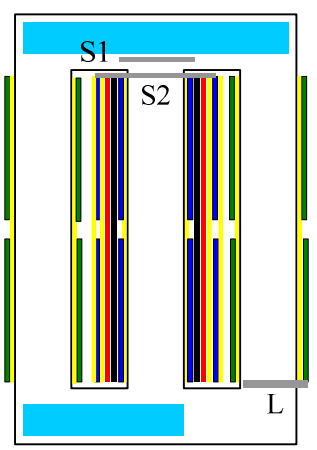

Fig. 8 Winding arrangement

center leg width is similar to the one of outer leg unlike the conventional core. The commercial PL-9 core material is selected.

The magnetic design is based on current density 450 A/cm^2. Fig. 8 shows the winding arrangement

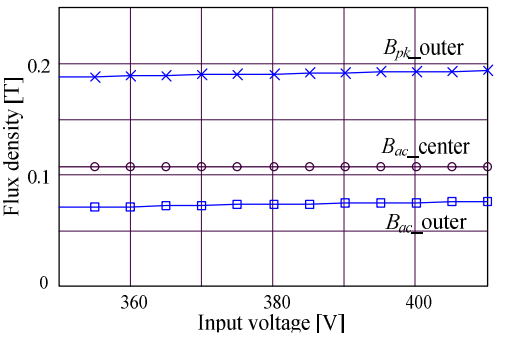

(a)

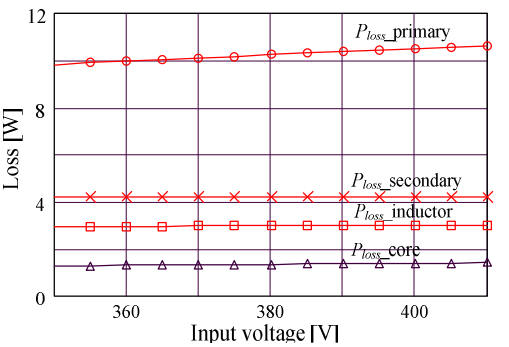

(b)

Fig. 9 Performance for input voltage variation, (a) flux density, (b) power loss

of proposed IM, where the primary and secondary windings are wound on the center leg and the output inductor are wound on two outer legs.

▫ Primary winding

- Number of turns : 40 turns, round wire
- Copper diameter: 0.85 mm
- Resistance: R_{DC}=0.086W, F_R=3.162

▫ Secondary winding

- Number of turns :2 turns, sheet wire
- Copper width & breadth: 17 mm & 0.6 mm
- Resistance: R_{DC}=0.478mW, F_R=2.487

▫ Inductor winding

- Number of turns : 2 turns, sheet wire
- Copper width & breadth: 17 mm & 1 mm
- Resistance: R_{DC}=0.287mW, F_R=4.182

F_R means the AC resistance factor derived from Dowell's curve.

3.2 Characteristic analysis

The analysis program is made by using MathCad tool. The performance is analyzed for both input

voltage and load variations.

Fig. 9 shows the flux density in the core and power loss for the input voltage variation from 340 V to 420 V. There is no dc flux in the center leg, so that the peak flux density is equal to the ac flux density magnitude. On the other hand, the dc and ac fluxes flow in the outer leg. The peak flux density in outer leg is higher than the one in center leg even though the width of center leg is reduced to half of the conventional core. The peak flux density is lower than 0.2 T for input voltage variation. The core loss is much smaller than the copper loss. The copper loss in the primary winding is highest among the power loss in the IM transformer and slightly increases with higher input voltage.

Fig. 10 shows the flux density in the core and power loss for the load variation from 300 W to 1.4 kW. The output inductor current increases with higher load, so that the peak flux density of the outer leg linearly increases. On the other hand, the flux density in the center leg is constant in spite of the load variation because the transformer flux density depends on the primary voltage-second product. The core loss is small and constant in spite of load variation. The copper loss is bigger than the core loss and rapidly increases with higher load.

The flux density in the center leg is much lower than one in the outer leg even though the center leg width is much reduced. This means that the center leg width can be more reduced. The external appearance of proposed IM is shown in Fig. 11. Its dimension is 52.1×38.0×29.2 in mm and the volume is 57.8 cm^3.

Fig. 12 shows the electrical waveforms for the proposed IM transformers. For blocking the dc current flowing through the primary winding, a blocking capacitor of 1 mF is connected in series with the primary winding. Since the magnetizing path includes air gap, the magnetizing inductance becomes lower, so that the peak primary current increases. However, the effect of magnetizing inductance is less significant when the load increases. The magnetizing coupling of the proposed IM transformer is better because the transformer is closely wound on the center leg, so the leakage inductance is small.

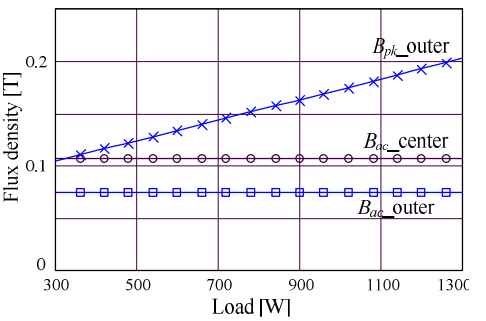

(a)

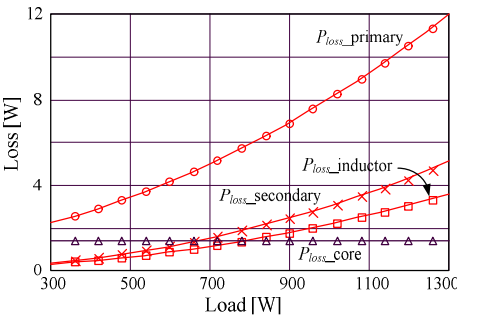

(b)

Fig. 10 Performance for load variation, (a) flux density, (b) power loss

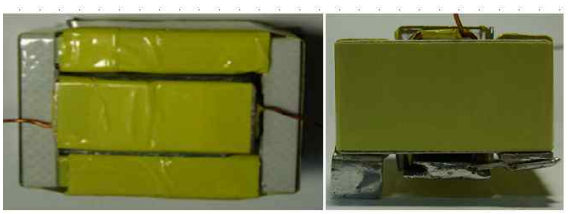

Fig. 11 External appearance

(a) 20 A load

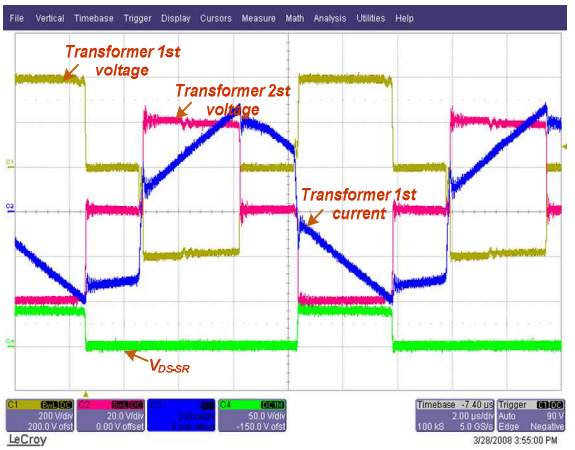

(b) 50 A load

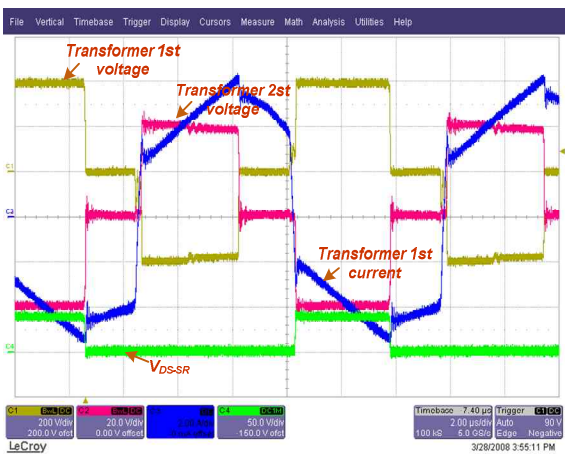

(c) 80 A load

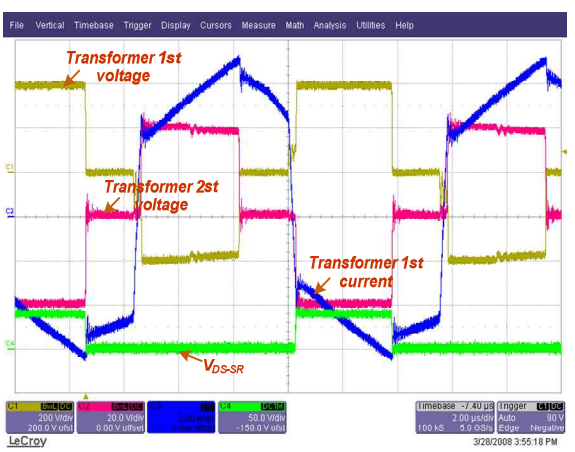

(d) 100 A load

Fig. 12 Experimental waveforms according to load variation (time: 2 ms/div, primary current: 2 A/div., primary voltage: 200 V/div., secondary voltage: 20 V/div.)

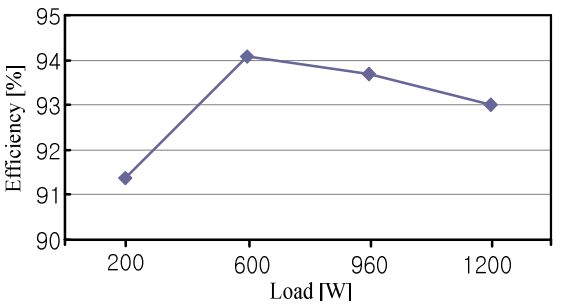

Fig. 13 Efficiency of ZVS PSFB converter with proposed IM transformer

Fig. 13 shows the experimental efficiency of the ZVS PSFB converter including the switching loss and IM transformer loss etc. The efficiency is calculated by dividing the measured output power by the measured dc link input power. The efficiency is about 94 % at half load and 93 % at full load. When the load is below 200 W, the efficiency becomes poor because of the hard switching instead of ZVS.

4. Conclusions

The IM transformer for ZVS phase shift full bridge converter is proposed and analyzed. The transformer and output inductor are integrated in one magnetic core. The transformer winding is located on the center leg of E-core for close magnetic coupling and the inductor is wound on two outer legs in series connection. An E-core is redesigned and implemented. The flux density equations are derived during each cycle in PSFB converter. The magnetic loss and performance are analyzed. With the proposed IM transformer, the converter efficiency of about 93 % is obtained at full load of 1.2 kW. The volume of IM transformer can be reduced, so that the power density can be increased.

References

[1] L. Yan, D. Qu, and B. Lehman, “Integrated magnetic full wave converter with flexible output inductor”, *IEEE Trans. Power Electron.*, Vol. 18, No. 2, pp.

670-678, Mar. 2003.
[2] P. Xu, Q. Wu, P. L. Wong, and F. C. Lee, "A novel integrated current doubler rectifier", *Proc. IEEE APEC'00*, Vol. 2, pp. 735-740, Feb. 2000.
[3] R. T. Chen and Y. Y. Chen, "Synthesis and design of integrated-magnetic-circuit transformer for VRM application", *IEE Proc.-Electr. Power Appl.*, pp. 369-378, Vol. 153, No. 3, May 2006.
[4] L. P. Wong, D. K. Cheng, M. H. L. Chow, and Y. S. Lee, "Interleaved three-phase forward converter using integrated transformer", *IEEE Trans. Ind. Electron.*, Vol. 52, No. 5, pp. 1246-1260, Oct. 2005.
[5] L. Yanand B. Lehman, "A capacitor modeling method for integrated magnetic components in DC/DC converters", *IEEE Trans. Power Electron.*, Vol. 20, No. 5, pp. 987-996, Sept. 2005.
[6] M. E. Eaton, "Adding flux paths to Spice's analytical capability improve the ease and accuracy of simulating power circuits", *Proc. IEEE APEC' 98*, pp. 386-392, 1998.
[7] B. Andreyecak, "Designing a phase shifted ZVT power converter", Unitrode Switching Regulated Power Supply Design Seminar Manual, pp. (3)1-15, 1993.

저 자 소 개

이형란(李馨蘭)
1982년 10월 28일생. 2006년 8월 遼宁科技大學 전기공학과 졸업. 2008년 8월 경상대 전기공학과 졸업(석사). 2008년～현재 동 대학원 전기공학과 박사과정.

신용환(辛龍桓)
1981년 12월 4일생. 2007년 3월 경상대 공과대학 전기공학과 졸업. 2009년 2월 경상대 전기공학과 졸업(석사). 2009년～현재 동 대학원 전기공학과 박사과정.

원재선(元載善)
1973년 2월 20일생. 1999년 영남대 대학원 전기공학과 졸업(석사). 2005년 영남대 대학원 전기공학과 졸업(공박). 2001년～2004년 영남대 공업기술연구소 연구원. 2004년～2006년 HSL 일렉트로닉스 전자설계팀 선임연구원. 2006년～현재 삼성전기 CDS사업부 Power선행개발G 책임연구원.

김종선(金鍾宣)
1981년 연세대 재료공학과 졸업. 1983년 연세대 전자재료공학과 졸업(석사). 1988년 동 대학원 전자재료공학과 졸업(공박). 1988년～1995년 삼성코닝(주) 연구소 선임연구원. 2004년～2009년 삼성전기(주) Power 사업팀 상품기획 그룹장. 2009년～현재 삼성전기(주) CDS사업부 사업기획 그룹장.

신휘범(愼輝範)
1982년 서울대 전기공학과 졸업. 1985년 한국과학기술원 전기 및 전자공학과 졸업(석사). 1992년 동 대학원 전기 및 전자공학과 졸업(공박). 1990년～1993년 현대전자(주) 선임연구원. 2000년～2002년 미국 University of Wisconsin Madison 방문교수. 1993년～현재 경상대 전기공학과 교수. 당 학회 협력이사.